Received: 10 July 2019 | Revised: 18 December 2019 | Accepted: 19 December 2019

DOI: 10.1002/jbio.201960033

JOURNAL OF BIOPHOTONICS

FULL ARTICLE

SERS-based biosensor for Alzheimer disease evaluation through the fast analysis of human serum

Cristiano Carlomagno | Monia Cabinio | Silvia Picciolini | Alice Gualerzi | Francesca Baglio | Marzia Bedoni*

Santa Maria Nascente Hospital, IRCCS Fondazione Don Carlo Gnocchi, Milan, Italy

***Correspondence**
Bedoni Marzia, Laboratory of Nanomedicine and Clinical Biophotonics, IRCCS Fondazione Don Carlo Gnocchi, Via Capecelatro 66, 20148 Milano, Italy.
Email: mbedoni@dongnocchi.it

Funding information
Italian Ministry of Health, Grant/Award Number: Ricerca Corrente 2016-2018

Abstract

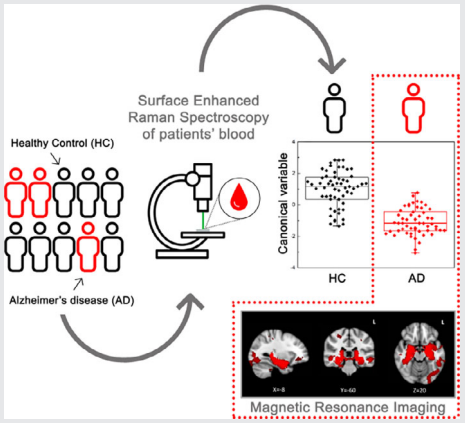

Alzheimer disease (AD) is the most common form of dementia in the elderly, progressively affecting the cognitive functions with a complex diagnostic procedure that limits the time for a prompt intervention. In this study we optimized a reliable protocol for the analysis of AD patients and healthy subjects' serum using the Surface Enhanced Raman Spectroscopy (SERS), taking into consideration the effect of different variables on the final spectra, analyzed and compared through multivariate analysis and correlated with hippocampus volume. As results, we demonstrated a statistical difference between the spectra collected from the two investigated groups, with an accuracy, precision and specificity of respectively 83%, 86%, and 86%. The correlation of these data with those obtained from MRI, demonstrated a direct correlation between Raman spectra and hippocampus degeneration showing the Raman Spectroscopy (RS) as a potential tool for the monitoring of AD progression and rehabilitation treatments.

KEYWORDS

Alzheimer, biomarkers, biosensor, MRI, SERS

1 | INTRODUCTION

Alzheimer disease (AD) is a common neurodegenerative disorder manifesting with progressive decline in cognitive functions (i.e., memory, thinking, comprehension, language). It is commonly accompanied by deterioration in emotional control, social behaviour or motivation, involving various potential biological and environmental factors. It is the most common cause of dementia in the elderly (>65 years old), affecting nearly 35.6 million people worldwide and this number is expected to double by 2030 and more than triple by 2050, thus making AD a public health priority [1]. Histopathologically the brain tissue of AD patients in its typical form is affected by neurodegeneration starting from the hippocampal region, leading to extensive atrophy in the cortical gray matter and accompanied by extracellular deposition of senile plaques. Considering the main commonly regarded AD hallmarks, senile plaques, and neuronal intracellular fibrillary tangles are made up of protein aggregates of

beta-amyloid (Aβ) and hyperphosphorylated tau protein, respectively [2].

Currently, there is no treatment able to stop or reverse the disease progression; however, some medications can relieve symptoms but their effect is strongly related to the promptness of treatment. In this context, the possibility to monitor the disease progression in a personalized and noninvasive way is desirable.

Nowadays a classification of the major biomarkers used in AD research was proposed dividing them into three categories based on the nature of the underlying pathophysiology: those related to the Aβ fibrillary deposition, those focused on the role of tau in forming neurofibrillary tangles, and those describing the neurodegeneration process, leading to a multidomain biomarkers profile (ATN classification) [3, 4]. Due to the high invasive procedure and the time used to obtain such biomarkers (i.e. cerebrospinal fluid and positron emission tomography/single-photon emission computer tomography PET/SPECT) and to improve the differential diagnosis between AD and other clinical forms of dementia of the elderly [5] the development of rapid, sensitive, noninvasive procedures for the detection of biomarkers related to the early onset and the progression of the disease remains a major challenge.

In the search for novel biomarkers that can be treated as continuous variable in relationship with brain damage [6–8], the Raman Spectroscopy (RS) analysis of serum can represent a valuable integration of the ATN system, moving AD research closer to personalized medicine by coding pathologic changes in a spectroscopic profile for each subject, that combined with genetic and clinical information, can be useful in tailoring pharmacological and rehabilitation treatments.

RS is a nondestructive, reagent, and label-free technique that can rapidly provide an overview of the chemical bonding and molecular structures of a sample. Because of the limited sample preparation required, RS was already proved to be effective in cancer diagnosis by the analysis of tissues [9] and cells [10] and also in the neurodegenerative field as recently reviewed by Devitt et al. [11]. What makes neurodegenerative disorders suitable for the RS approach is the central hallmark of most diseases, that is, the protein misfolding and aggregation, that can alter the Raman spectrum providing information about the structural organization of amyloid fibrils [12]. In the AD research field, RS has been applied to the investigation of human brain tissue post-mortem [13], as well as platelets and blood samples [14, 15], demonstrating the potentiality of the methodology on patients' biofluids, although limited by the sensitivity of the detection method. To overcome this issue, *Surface Enhanced Raman Spectroscopy (SERS)* strategies were developed, in order to detect Aβ [16] and tau protein [17] thanks to the contribution of nanostructures. In particular antibody-based detection methods were used with increased signal enhancement and rapidity compared to commercially available ELISA kits [18].

In the present work, we introduce an innovative SERS-based biosensor to analyze the human serum, that minimizes the use of reagents, avoids antibodies and relies on a continuous variable, that is, the SERS spectrum, testing its feasibility in a pilot sample of AD patients well characterized from a ATN perspective. After the optimization of nanoparticles synthesis, sample processing and acquisition settings, multivariate statistical analysis was performed and the resulting classification model has demonstrated that SERS data correlate with well-established neural injury biomarkers for AD, that is, magnetic resonance imaging (MRI) total hippocampal volume, introducing for the first time a promising SERS-based method in the AD field.

2 | MATERIALS AND METHODS

2.1 | Patients recruitment, clinical, and MRI evaluation

Ten subjects with AD (three males, seven females, 73 ± 2.7 age) were recruited at the Unit of Rehabilitative Neurology of IRCCS Fondazione Don Carlo Gnocchi after ethics committee approval. The male/female patients' ratio was selected due to the female prevalence in epidemiology of AD, selecting a representative cohort of AD patients with a female prevalence (group gender distribution not statistically different, chi-square test, $P = .7990$) [19]. The study was conducted following the declaration of Helsinki criteria and the guidelines for good clinical practice of the European Medicines Agency. All persons involved in this study gave their informed consent prior to their inclusion. The inclusion criteria were: (a) probable AD according to ATN criteria [3, 4] with an amyloid-PET scanning session (18F-Florbetapir), in order to test for Aβ burden; (b) mild stage of the disease with a Clinical Dementia Rating (CDR) scale score between 0.5 and 1 [20]; (c) absence of MRI contraindications or brain abnormalities.

Moreover, a group of 11 healthy controls (HC; four males, seven females, 65.6 ± 4.9 age) was enrolled in the study and submitted for signature of informed consent in accordance with the ethical principles of the Declaration of Helsinki. HC did not have a family history of dementia, evidence of neurologic or systemic diseases at the time of enrolment. Table 1 reports the main characteristics of the subjects involved in the study.

TABLE 1 Main characteristics of the subjects recruited for the study

		AD	HC
Number		10	11
Gender	Males	3	4
	Females	7	7
Age (mean ± SD)		73 ± 2.7	65.6 ± 4.9
Scolarity (mean ± SD)		11.7 ± 4.6	14.3 ± 3.7
MoCA (mean ± SD)		19.2 ± 3.1	23.6 ± 2.5
Global CDR		8 subjects 0.5; 2 subjects 1	

At recruitment, all subjects were asked to complete Montreal Cognitive Assessment (MoCA) [21] scale, in order to test the cognitive status and MRI examination. MRI protocol (1.5T Siemens Magnetom Avanto) included the following sequences: (a) conventional sequences (FLAIR, T2-weighted), in order to exclude brain abnormalities; (b) 3D T1-weighted magnetization prepared rapid gradient echo (TR = 1900 ms; TE = 3.37 ms; TI = 1100 ms; flip angle = 15°; 176 contiguous, 1 mm thick axial slices; matrix size = 192 × 256; FOV = 192 mm × 256 mm), to evaluate brain morphometry. Volumetric evaluation of total intracranial volume and hippocampus were performed using Freesurfer image analysis suite (http://surfer.nmr.mgh.harvard.edu/), according to Desikan atlas [22]. The brain morphometrical measures of brain atrophy are reported in Table 2. Cortical segmentations have been visually inspected according to ENIGMA pipeline (http://enigma.ini.usc.edu/protocols/imaging-protocols), to ensure quality segmentation. Hippocampal volumes were computed using a dedicated Freesurfer pipeline, according to Iglesias et al [23]. Direct between-group statistical comparisons have been performed on left, right and total (left + right) hippocampal volumes (ANCOVA analyses, including total intracranial volume as covariate), in order to highlight the specific marker of neural downstream degeneration in our AD sample.

Measure of cortical thickness of a brain region not involved in AD pathology (left post-central gyrus) was included as control region. A between group comparison (ANOVA) was performed. Results have been considered as statistically significant when surviving $P < .05$ threshold. In order to investigate the whole brain pattern of atrophy in our sample, a between-group whole brain comparison was also performed using a voxel-wise method (fslVBM). Results have been considered as statistically significant when surviving the 0.001 threshold (TFCE corrected).

2.2 | Sample collection

Human peripheral blood samples of each subject were collected in BD Vacutainer SST II Advance tubes. After the clotting time of 60 minutes, samples were centrifuged 2500*g* × 10 min at room temperature, anonymized, aliquoted and stored at −80°C until further use.

2.3 | Synthesis and characterization of Ag and Au nanoparticles

Ag and Au nanoparticles (NPs) were synthesized in order to be used for the SERS analysis of the serum. AuNPs were produced following the Frens's method [24]. Briefly, 200 mL water solution of 0.01 wt% $HAuCl_4 \cdot 3H_2O$ was heated under stirring until boiling. Then, 1.4 mL of sodium citrate was quickly added, the solution was cooled and stored at room temperature.

AgNPs were synthesized according to the Lee-Meisel procedure [25]: 10 mL of 1 mM silver nitrate was slowly added to 30 mL of 2 mM sodium borohydride solution under vigorous stirring. The AgNPs solution is stable for some months and could be stored at +4°C.

TABLE 2 Brain morphometrical measures of brain atrophy

	AD	HC	*P* value
Hippocampal volume (mm^3, mean ± SD)[a]			
Right	2366.868 ± 250.1316	3465.023 ± 409.1191	*<.001*
Left	2086.375 ± 149.3956	3389.188 ± 400.8063	*<.001*
Total (right + left)	4453.243 ± 364.1531	6854.213 ± 801.742	*<.001*
Left post-central gyrus thickness (mm)[§]	1.76 ± 0.19	1.85 ± 0.15	.198
Total intracranial volume (mm^3)[b]	1 467 959.47 ± 113316.82	1 513 629.86 ± 162 159.40	.447

Results are considered as statistically significant when surviving $P < .05$ threshold.
[a]ANCOVA.
[b]ANOVA.

Synthesized selected nanoparticles were characterized for dimension, stability and Raman signal using a nanodrop UV–Vis 2000c spectrometer (Thermo Scientific), Auriga Compact Field Emission—Scanning Electron Microscope with accelerating voltage ranging in 5 to 15 kV (Zeiss, Germany), NanoSight NS300 Instrument (Malvern, UK) and a Raman microscope (LabRAM Aramis, Horiba Jobin Yvon S.A.S, Lille, France). The chemicals used for these protocols were purchased by Sigma Aldrich and used as received.

2.4 | SERS measurements

Raman and SERS analyses were performed by using a Raman microscope (LabRAM Aramis, Horiba Jobin Yvon S.A.S, Lille, France) equipped with a laser source operating at 785 nm. For each measurement, a drop of 5 μL of sample was lied on a CaF_2 slide; 6 spectra were collected following a line-map from the edge to the center of the same drop in the region between 400 and 1800 cm^{-1}, with acquisition time of 30 s and a ×50 objective. Laser power was set to 100% (512 mW) for all the acquisitions. We tested different protocols for the preparation of the serum samples in order to optimize the methodology (discussed in the results paragraph as "methodological study") and obtain the standard parameters for the Raman analysis of the serum before the pilot application with AD samples. In particular, we collected the Raman spectra of pure serum and of serum after filtration with 3, 10, or 30 kDa filters, and the SERS spectra of the serum mixed with AgNPs or AuNPs, at different concentrations (NP:serum, 9:1 and 5:1) and times of incubation (0, 15, 30, 45, and 60 min). These experiments for the optimization of the SERS protocol were conducted using serum samples of the HC subjects.

Then, all the serum samples of AD patients and HC were analyzed following the optimized protocol for SERS spectra acquisition and data were collected through LabSpec6 software (Horiba Scientific).

2.5 | Statistical analysis

After removal of a third-order polynomial baseline, each SERS spectrum was normalized through unit vector normalization using LabSpec6. The normalized data were analyzed by multivariate statistical analysis using Origin2018 software (OriginLab, Northampton, MA). Principal component analysis (PCA) of the normalized spectra provided principal components (PCs) representing the differences in serum SERS spectra. Linear discriminant analysis (LDA) was applied to discriminate and classify spectra from AD and HC. The sensitivity, specificity and accuracy of the LDA model were tested using leave-one-out cross-validation performing the analysis on the single spectra acquired. One-way ANOVA was then performed on PC scores to verify the statistical significant differences between the groups. The statistical correlations between SERS, MRI and clinical data were evaluated by means of Mann-Whitney, Pearson's, partial correlation and covariance test. In particular correlation and partial correlation between collected data were performed using origin software. The canonical variable (CV) obtained from multivariate analysis were directly correlated with MoCA scores of the AD patients. The partial correlations were performed between CV and cortex thickness left, right and whole hippocampus volumetric data covariated for age and intracranial volume (Pearson's test).

3 | RESULTS AND DISCUSSION

3.1 | Methodological study

In the first part of the study, we evaluated the impact of the processing of HC serum samples using (a) filters with different cutoff and (b) the application of two nanostructures in order to achieve the optimal SERS effect. These two steps (filtering and NP application) were finalized to obtain the maximum detail from the resultant Raman spectra before the analysis of AD serum samples. The filtration step is usually adopted before the RS analysis of biological fluids, to exclude from the analysis impurities or molecules with an intense Raman signal, that is expected to hide the one from critical small metabolites and other small moieties. In Figure 1, average spectra (±1 SD) obtained from pure serum (unfiltered) and serum processed using filters with cutoff of 3, 10, and 30 kDa are shown. The spectrum of pure serum showed a noisy and poorly detailed signal, dominated by protein-related bands [26]. After filtration and removal of a part of the serum proteins with the three types of filters, the Raman spectra showed more defined and intense peaks still attributable to proteins (Figure 1), in particular at 1450 cm^{-1} (CH_2/CH_3 deformations), at 1127 and 853 cm^{-1} (Tyrosine) and 1250 cm^{-1} (amide III band). Because of the large spectral interference of the proteins, the introduction of nanostructured systems for the detailed analysis of human serum was necessary. In order to achieve the SERS effect, we tried to mix serum with two different standard metal NPs already used as SERS inducers for RS of serum: spherical AuNP and AgNPs [26]. In Figure 2A, the comparison between 3 kDa-filtered serum without NPs and 3 kDa-filtered serum mixed with AuNPs or AgNPs (NPs:serum ratio 9:1) is shown.

The effect of NPs on unfiltered serum was not tested due to the well-known "protein corona" effect, in which specific serum proteins, for example, albumin, immediately aggregate on nanostructured metallic surfaces inducing a steric repulsion which inhibits the NPs aggregation and, consequently, the SERS effects [27]. On the contrary, using filtered serum (3 kDa) coupled with AgNPs or AuNPs two distinct interactions between serum components and NPs are visible. AuNPs are not able to induce the SERS effects, probably due to the missing aggregation of the metallic nanostructures with molecules present in serum. On the other hand, the introduction of AgNPs is able to induce a strong SERS effect probably caused by partial or total aggregation with serum proteins, forming the NP-clusters with plasmonic properties suitable for the SERS application [28]. AgNPs were characterized for dimension, stability and Raman background, showing a good dimensional monodispersion, low nanoparticles degradation rate and low Raman signal contribute when analyzed with and without serum (Figures S1, S2, and S3). In particular, AgNPs showed an average diameter of 45 nm with a high concentration of particles/ml with a diameter of 35 nm, after characterization using Scanning Electron Microscopy and Nanoparticles Tracking Analysis (Figure S1A). The stability, Raman background and the potential degradation of used AgNPs were estimated using UV–Vis and Raman Spectroscopy (Figures S1B, S2, and S3). All the performed analysis demonstrated the weak Raman background of pure AgNPs (Figure S2A and B) and the low

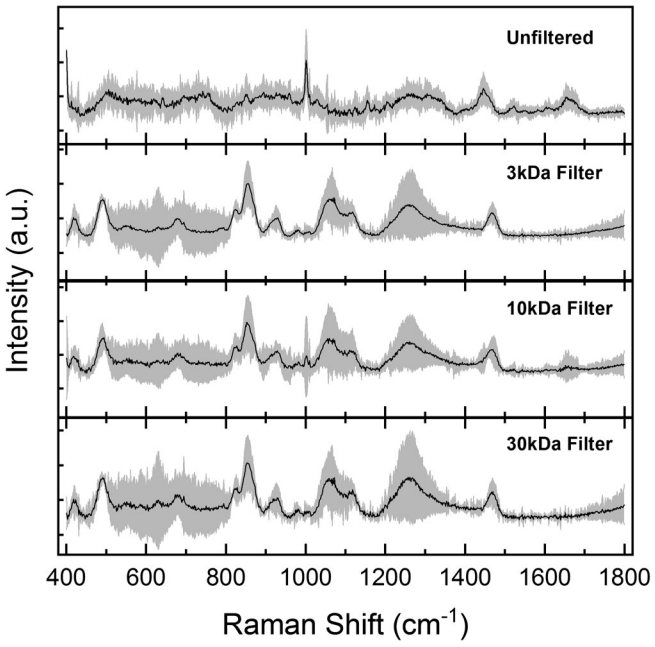

FIGURE 1 Normalized Raman spectra of human serum unfiltered and filtered with cutoff of 3, 10, and 30 kDa. The black lines are the average of the acquired maps, while the gray bands are the SD

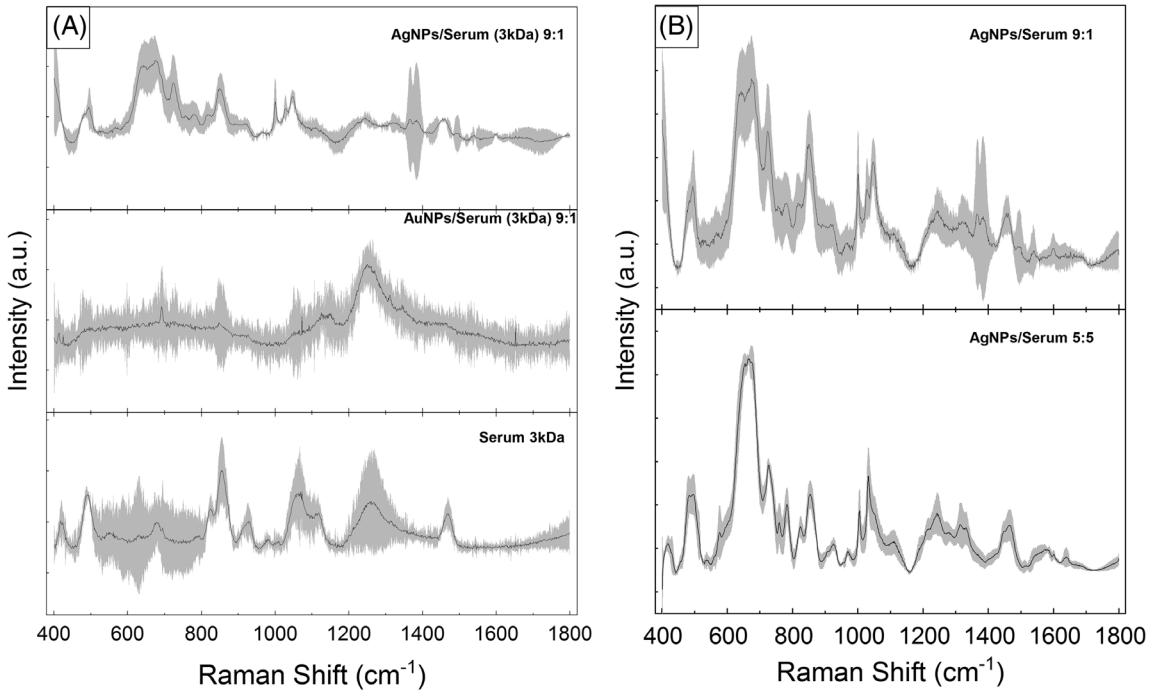

FIGURE 2 A, Normalized SERS spectra of silver nanoparticles [AgNPs/Serum (3 kDa) 9:1] and gold nanoparticles [AuNPs/Serum (3 kDa) 9:1] mixed with human serum filtered with a 3 kDa cutoff with a ratio of 9:1 and Raman spectra of human filtered serum on CaF_2 (Serum 3 kDa). B, Normalized SERS spectra of filtered human serum mixed with silver nanoparticles with a ratio of 9:1 (AgNPs/Serum 9:1) and 5:5 (AgNPs/Serum 5:5). The gray bands identify the spectra SD

degradation rate of AgNPs and the consecutive ability to achieve the SERS effect also after 8 days (Figure S3).

Obviously, the cluster formation and consequent SERS induction depends on both serum and NP concentrations. For this reason, we tested different AgNPs to serum ratios, evaluating possible changes in the resultant Raman spectra (Figure 2B). The ratio 9:1 was selected for further experiments due to the presence of more detailed SERS spectra compared to the one obtained with a ratio of 5:5, despite higher SD. Two regions in the 9:1 ratio presented a higher detail compared to the 5:5 ratio: the peak at 663 cm^{-1} and the region between 1480 and 1700 cm^{-1}. As a result, we can speculate that the AgNPs to serum ratio of 9:1 induced the formation of clusters, composed of NPs and serum proteins, able to induce an optimal increase of electromagnetic field which is responsible of the enhancement of the Raman signal. Finally, the process of nanostructured cluster formation in an aqueous system is dependent not only on the concentrations of the molecules involved, but also on the incubation time. In order to test this variable, we performed Raman analysis on AgNPs and serum mixtures incubated for 0, 15, 30, 45, and 60 min at room temperature (Figure 3). Increasing the incubation time, spectra revealed an increase both in spectrum detail and in the analysis uniformity (lower SD values, Figure 3 gray band). Also this result is amenable to the cluster formation, being a possible explanation the progressive formation of protein aggregates on the NPs surface and consecutive achievement of a stable and optimal state at T45 (Figure 3). To maximize the spectral yield decreasing the relative SD, we decided to perform the further analysis after an incubation time of 45 min. In conclusion, we decided to set the filter with 3 kDa cutoff, AgNPs to serum ratio at 9:1 and 45 min of incubation at room temperature for the further analysis of HC and AD serum samples, thus ensuring detailed SERS spectra with only partial protein removal. The evaluation of all the analytical process parameters, as well as the characterization of a systemic protocol for the serum analysis, are fundamental to obtain reliable and reproducible measurements. Our procedures require few steps, leading in about 1 h (including AgNPs synthesis, when necessary) to the Raman data collection and processing.

3.2 | SERS clinical data

To assess the feasibility of the SERS-based biosensor on clinical samples, serum samples of 10 AD and 11 HC

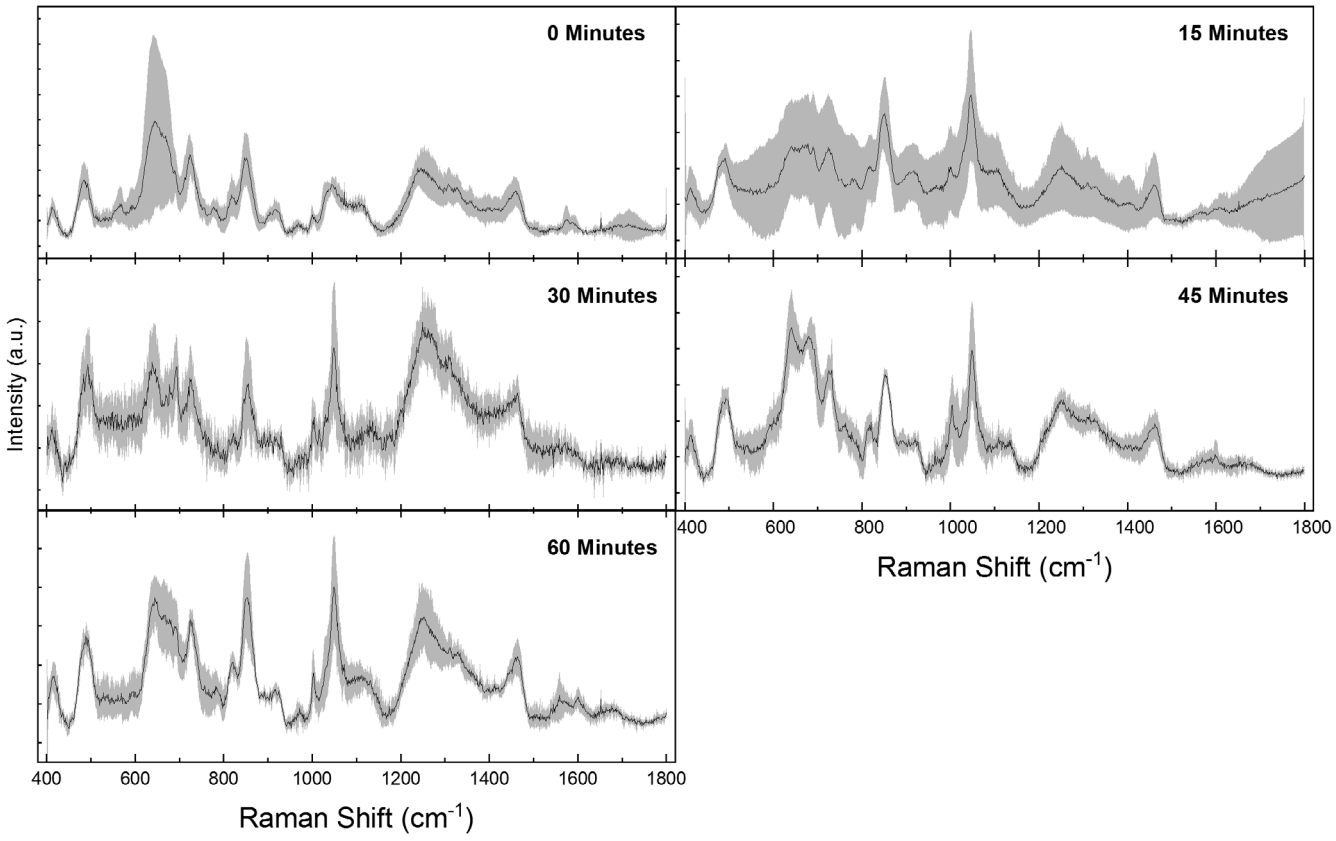

FIGURE 3 Normalized SERS spectra of silver nanoparticles mixed with filtered human serum with a ratio of 9:1 with 0, 15, 30, 45, and 60 min of incubation before the Raman analysis. The gray bands identify the spectra SD

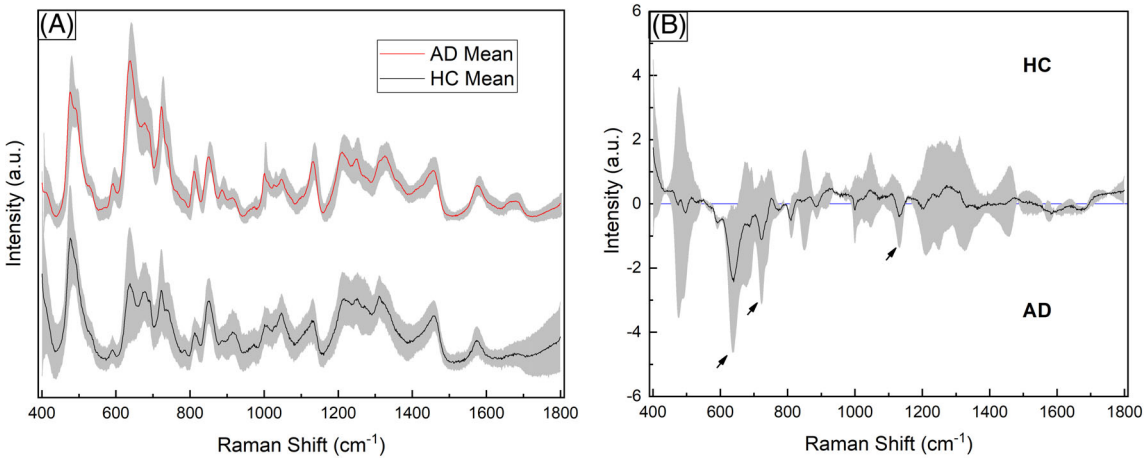

FIGURE 4 A, Average SERS spectra with SD of healthy controls (HC Mean) and patients with Alzheimer's disease (AD Mean). The gray bands identify the spectra SD. B, Resultant differences between the average spectra acquired for HC and AD. Black arrows indicate the partially attributed peaks. The gray band indicates the error propagation

were analyzed. In Figure 4, the average spectra of the AD and HC group (six spectra per sample, Figure 4A) and the subtraction spectrum between the two groups (Figure 4B) are reported. The main differences, highlighted in Figure 4B, in terms of intensities were related to specific peaks identifiable as ascorbic acid (591 cm^{-1}), hypoxantine (724 cm^{-1}), and uric acid (634 and 1128 cm^{-1}) [29]. In particular, the intensities of the above cited peaks were found to be higher, with the associated error propagation, in the AD subjects respect to the HC group, suggesting a variation in the serum content of these molecules and thus in the cellular metabolism (Figure 4B, black arrows). Our Raman data on hypoxantine (Figure 4B, peak at 724 cm^{-1}), which is the principal purine nucleobase involved in the brain's salvage pathway, support previously reported data about the activity of the enzyme hypoxantine-guanine phosphoribosyltrasferase (HPRT) in AD pathogenesis [30]. HPRT activity was demonstrated to be decreased in AD, leading to the progressive accumulation of hypoxantine [30], as confirmed by our Raman observations. HPRT decreased activity was also associated to the accumulation of uric acid (Figure 4B, peaks at 634 and 1128 cm^{-1}) [31], which is a widely studied natural antioxidant associated with dementia, cognitive functions loss and Alzheimer. Despite being in line with previous data about the role of oxidative stress in AD pathogenesis [32], we cannot exclude that the differences, in particular the increase in ascorbic acid concentration (Figure 4B, peak at 591 cm^{-1}), related to specific peaks might be related more to the vitamin supplements and medical nutrition products (ie, with supplement of docosahexaenoic acid, eicosapentaenoic acid, uridine monophosphate and choline, B-vitamins, vitamin C, E, selenium, and phospholipids) taken by AD patients than to an AD-related variation. For this reason, deeper studies are required to characterize the effects of the used drugs on the complete serum biochemistry involving a controlled cohort of patients to ascertain the origin of ascorbic acid, hypoxanthine and uric accumulations. This preliminary Raman analysis is able to provide a rapid potential indication about the biochemical differences in the two considered groups, opening the way for specific and addressed further biochemical analysis. The statistical differences between the two groups were analyzed using PCA-LDA. The introduction of unsupervised statistical analysis, allows to the reduction of complex datasets into small numbers of orthogonal PCs (statistically independent). PCs accounts for the variations between the datasets analyzed, which contains the Raman features responsible for the best variation between the spectra. Increasing the data analysis and statistical complexity could be also possible to attribute the biochemical sources of variation between, for example, a pathological or physiological state [33]. Figure 5A shows the score plot of PC1 (35.1%) and PC2 (20.6%) with the grouping of the values identified for each group (confidence interval 95%). In the plot, the AD values are grouped in a defined region respect to the HC group that are more dispersed, suggesting a smaller intra-group variability among AD samples. A probable explanation for this grouping can be found in the high presence of disease-related molecules such as mutated protein, growth factors, mediators of the inflammatory response, protein and lipids with an attributed role of neuroprotectors, nucleic acids and other, induced by the disease onset [34–38]. The first 10 PC scores were then used to obtain the canonical variable 1 (CV1) that allowed the classification of the spectra. The

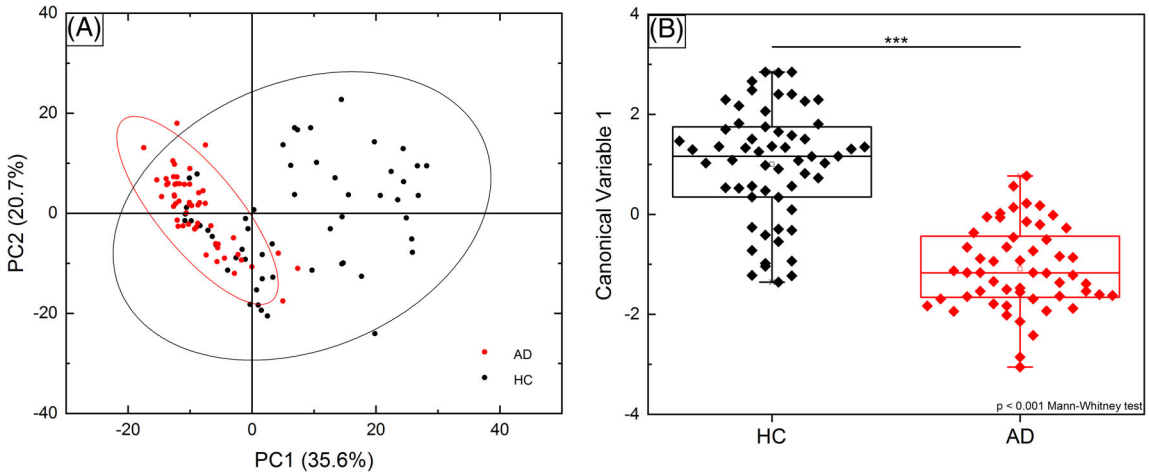

FIGURE 5 A, Principal component analysis of data, with the 95% confidence interval ellipse, and B, linear discriminant analysis acquired from 10 AD and 11 HC. $P < .001$ Mann-Whitney test

CV1 values obtained for AD and HC were compared with the nonparametric Mann-Whitney test (Figure 5B) demonstrating a statistical difference ($P < .001$) and thus confirming the ability of RS to distinguish between the two group of subjects. Although preliminary and on a limited number of patients, the accuracy, precision and specificity were calculated from the cross-validation test for each single spectrum acquired (126 AD and HC acquired spectra) with values of respectively 83%, 86%, and 86%. RS has already been proposed as potential tool for AD diagnosis, in particular the most common trend was to perform the analysis directly on human (post-mortem) or animal brain tissue or investigating the effects of drugs on Aβ fibrils in vitro [39–41]. The main advantage of our SERS-based method, respect to the others, is the possibility to perform the analysis with limited invasiveness for the patients. Using serum, the analysis can be performed many times after the diagnosis, monitoring for example the effects of the chosen therapy or of the rehabilitation course directly on the patient. The obtained results are coherent with other similar works presented in literature in which unfiltered serum was analyzed using conventional RS and multivariate analysis, through the application of a neural network, demonstrating the feasibility of the RS method. The analysis of serum allows to collect a whole overview of all the physiological and/or pathological biochemical composition, reflecting in this way the pathological mechanism. The information obtained in this way can easily confirm and discriminate the AD diagnosis also distinguishing AD from other neurodegenerative dementias, drastically decreasing the time for a differential diagnosis [42]. The methods applied from the cited researches allow a fast discrimination between the signal of AD patients and healthy subjects or patients with other neurodegenerative diseases but the information is finite to this output. In our work, through the multivariate analysis, we obtained a value uniquely attributable to the respective patient allowing the possibility to correlate this specific value to clinical and paraclinical tests. This correlation leads to an expansion of the information provided by Raman signals characterizing not only the disease onset and progression, but also for example the state of nervous system degeneration and dementia progression. In this way RS can be used not only for AD diagnosis, but also to monitor the nervous system degeneration and consequently the therapy effectiveness and the physical and cognitive rehabilitation, all fundamental to slow down the pathological progress [15, 42]. Nowadays the AD diagnosis is performed combining data obtained from different techniques of neuroimaging, mental status and neurophysiological test in a process that takes a considerable time [43]. The diagnostic technique based on RS takes about 1 h in a process (most of which in sample preparation that can be done simultaneously for a set of samples) that can be easily automatable. Once well validated, our methodology will potentially consolidate the outcome of the standard diagnostic process, giving overall information about the pathological onset, stratification and involved biochemical species.

3.3 | Neuroimaging data

The results of the between-group comparison considering right, left and total (right + left) hippocampal volume show a bilateral pattern of hippocampal atrophy in our AD sample, marker of neuronal downstream degeneration. No between-group differences were found when considering a control cortical region (left post-central

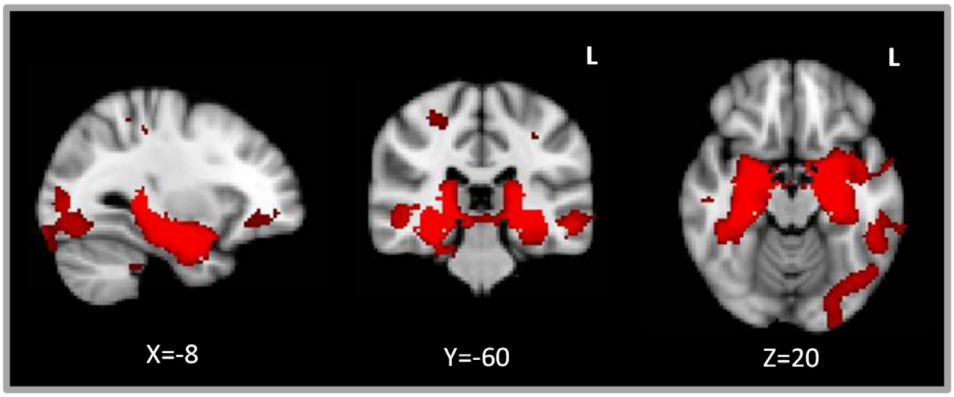

FIGURE 6 Whole brain between-groups comparison. In red colors are shown the cortical areas of cortical atrophy in AD patients when compared to HC subjects

TABLE 3 Partial correlation coefficients and relative P values correlated with left, right and mean hippocampus volumes (data obtained from MRI) and corrected for age and total intracranial volume (mm^3)

Canonical Variable 1	Left whole hippocampus	Right whole hippocampus	Whole hippocampus
Partial correlation coefficient	−0.566	−0.536	−0.558
P value	0.0011	0.0173	0.0012

$P < .05$, two-tailed test of significance.

gyrus) and in total intracranial volume. The investigation cerebral brain atrophy by means of a whole-brain analysis (fslVBM) shows a pattern in line with the diagnosis of AD, with cortical atrophy diffuse in brain areas mostly involving medial temporal region cortices and temporal lobe in the AD patients compared to HC. Whole brain comparison results are shown in Figure 6. To further verify the feasibility of the RS assay of serum coupled with the multivariate analysis for the identification of AD patients by means of a SERS-based biosensor, RS data were coupled with the results of MRI.

3.4 | Correlation between SERS and neuroimaging data

Data obtained from multivariate analysis of Raman spectra were correlated with data acquired from MRI analysis of HC and AD. The partial correlation of CV1 with hippocampus volumes were corrected for the subject ages and total intracranial volume, with partial correlation coefficient and *P* values showed in Table 3. CV1 presented a negative correlation for all the parameters taken into consideration with a significance less than 0.05 for all the measurements. Interestingly, the MoCA results were directly correlated with CV1 showing a missing correlation for values of Pearson's coefficient of −0.24 with a *P* value of 0.27. As further control, the CV1 values were partially correlated with cortex thickness using the age of the subjects as correction parameter. The correlation coefficient was −0.12 (*P* value = 0.6) confirming the independence of the CV1. The correlation between CV1 and hippocampus volume represents the most significant result of this work, being the hippocampus atrophy one of the well-known phenomena involved in AD progression. The identification of the correlation paves the way for future studies on the application of our SERS-based biosensor as useful tool for AD, with the CV1 being usable also as continuous variable for the monitoring of the neurodegenerative process. In this case, the CV1 was indirectly proportional to the hippocampus volume indicating that the RS of serum has the potential not only to recognize signs of AD onset, but also the degree of neuronal degeneration, by means of a fast technique and a minimally invasive procedure. Despite the single peak attribution is still challenging, the SERS spectra can be used as "whole biomarker" for the physiological or pathological state, providing an overview about biochemical state and all the biofluid components. The current study is not without limitations. The small sample size, between groups differences in pharmacological profiles and age range (Table 1), represents the principal pitfalls. An increased number of subjects is needed to definitely assess the potential of RS and a narrower age range of patients could improve the quality of the analysis, removing all the biochemical variables matched to the age of the subjects. Besides, a possible further step is the comparison between AD patients and other subjects affected by non-AD dementia including Lewy's body dementia, Parkinson's disease or frontotemporal dementia.

The correlation between Raman data and neuroimaging information, reveals a direct relationship between the brain tissue degeneration and the appearance of a specific biochemical pattern in serum collected from AD patients. This result is coherent with studies associating the detection of different blood biomarkers during the AD onset [44]. Taking advantage from RS, the overall differences in biochemical specimen can be detected and associated at the same time to a well characterized tissue modification, such as the brain tissue degeneration highlighted by MRI. Our results demonstrated the validity and reliability of RS not only for diagnostic purpose, but also as fast and simple monitoring tool for events associated to the pathological mechanism.

4 | CONCLUSIONS

In conclusion, our findings demonstrated the potential application of a SERS-based biosensor as a promising tool for the label-free analysis of serum samples collected with a minimal invasive way in subjects with AD. The RS analysis of serum was optimized introducing nanostructures in order to induce a SERS signal with more detailed and intense Raman spectra. All the analyzed parameters were standardized in order to achieve the best repeatability, minimizing the variables involved. After the methodological part, the optimized parameters were used for the analysis of serum collected from 10 AD and 11 HC. Interestingly, CV1 was correlated with hippocampal volumes suggesting a relationship with brain biomarkers of neural damage. To the best of our knowledge, it is the first time that the results obtained with an innovative, nanotechnology based biosensor are correlated to MRI results for the evaluation of AD patients, providing solid background for further investigation of its applicability in the monitoring of AD progression and rehabilitation treatments. The characterized Raman fingerprint represents a possible "whole biomarker" that contains information about the biochemical condition of the sample with an elevated translational potential for the noninvasive characterization of other neurodegenerative diseases.

ACKNOWLEDGMENTS

This study was supported by the Italian Ministry of Health, Ricerca Corrente 2016-2018 to IRCCS Fondazione Don Carlo Gnocchi.

CONFLICT OF INTEREST

The authors declare no conflicts of interest.

ORCID

Marzia Bedoni https://orcid.org/0000-0003-2618-3661

REFERENCES

[1] M. J. Prince, F. Wu, Y. Guo, L. M. Gutierrez Robledo, M. O'Donnell, R. Sullivan, S. Yusuf, *Lancet* **2015**, *385*(9967), 549. https://doi.org/10.1016/S0140-6736(14)61347-7.

[2] F. La Rosa, M. Saresella, F. Baglio, et al., *Sci. Rep.* **2017**, *7*(1), 16760. https://doi.org/10.1038/s41598-017-16754-y.

[3] C. R. Jack, D. A. Bennett, K. Blennow, et al., *Neurology* **2016**, *87*(5), 539. https://doi.org/10.1212/WNL.0000000000002923.

[4] C. R. Jack, D. A. Bennett, K. Blennow, et al., *Alzheimers Dement.* **2018**, *14*(4), 535. https://doi.org/10.1016/j.jalz.2018.02.018.

[5] N. Bogdanovic, *US Neurol.* **2018**, *14*(1), 15. https://doi.org/10.17925/USN.2018.14.1.15.

[6] M. Cabinio, M. Saresella, F. Piancone, F. LaRosa, I. Marventano, F. R. Guerini, R. Nemni, F. Baglio, M. Clerici, *J. Alzheimers Dis.* **2018**, *66*(3), 1131. https://doi.org/10.3233/JAD-180250.

[7] R. Mancuso, F. Baglio, S. Agostini, et al., *Front. Aging Neurosci.* **2014**, *6*, 285. https://doi.org/10.3389/fnagi.2014.00285.

[8] F. Baglio, M. Saresella, M. G. Preti, M. Cabinio, L. Griffanti, I. Marventano, F. Piancone, E. Calabrese, R. Nemni, M. Clerici, *Front. Aging Neurosci.* **2013**, *5*(NOV), 81. https://doi.org/10.3389/fnagi.2013.00081.

[9] M. Gniadecka, P. A. Philipsen, S. Sigurdsson, et al., *J. Invest. Dermatol.* **2004**, *122*(2), 443. https://doi.org/10.1046/j.0022-202X.2004.22208.x.

[10] R. Vanna, P. Ronchi, A. T. M. Lenferink, C. Tresoldi, C. Morasso, D. Mehn, M. Bedoni, S. Picciolini, L. W. M. M. Terstappen, F. Ciceri, C. Otto, F. Gramatica, *Analyst* **2015**, *140*(4), 1054. https://doi.org/10.1039/c4an02127d.

[11] G. Devitt, K. Howard, A. Mudher, S. Mahajan, *ACS Chem. Nerosci.* **2018**, *9*(3), 404. https://doi.org/10.1021/acschemneuro.7b00413.

[12] Z. Hu, X. Wang, W. Wang, Z. Zhang, H. Gao, Y. Mao, *Phys. Chem. Chem. Phys.* **2015**, *17*(35), 22711. https://doi.org/10.1039/c5cp02366a.

[13] Sudworth CD, Archer JKJ, Mann D. *Near infrared Raman spectroscopy for Alzheimer's disease detection*. In: Mycek M-A, ed, Diagnostic Optical Spectroscopy in Biomedicine III; 2005: 5862. doi:10.1117/12.633005

[14] P. Carmona, M. Molina, M. Calero, F. Bermejo-Pareja, P. Martínez-Martín, A. Toledano, *J. Alzheimers Dis.* **2013**, *34*(4), 911. https://doi.org/10.3233/JAD-122041.

[15] E. Ryzhikova, O. Kazakov, L. Halamkova, D. Celmins, P. Malone, E. Molho, E. A. Zimmerman, I. K. Lednev, *J. Biophotonics* **2015**, *8*(7), 584. https://doi.org/10.1002/jbio.201400060.

[16] W. A. El-Said, T.-H. Kim, C.-H. Yea, H. Kim, J.-W. Choi, *J. Nanosci. Nanotechnol.* **2011**, *11*(1), 768. https://doi.org/10.1166/jnn.2011.3268.

[17] A. Zengin, U. Tamer, T. Caykara, *Biomacromolecules* **2013**, *14*(9), 3001. https://doi.org/10.1021/bm400968x.

[18] T. Demeritte, B. P. V. Nellore, R. Kanchanapally, et al., *ACS Appl. Mater. Interfaces* **2015**, *7*(24), 13693. https://doi.org/10.1021/acsami.5b03619.

[19] M. M. Mielke, P. Vemuri, W. A. Rocca, *Clin. Epidemiol.* **2014**, *6*(1), 37. https://doi.org/10.2147/CLEP.S37929.

[20] B. Borroni, D. Perani, M. Broli, F. Colciaghi, V. Garibotto, B. Paghera, C. Agosti, R. Giubbini, M. Luca, A. Padovani, *J. Neurol.* **2005**, *252*(11), 1359. https://doi.org/10.1007/s00415-005-0867-z.

[21] Z. S. Nasreddine, N. A. Phillips, V. Bédirian, et al., *J. Am. Geriatr. Soc.* **2005**, *53*(4), 695. https://doi.org/10.1111/j.1532-5415.2005.53221.x.
[22] R. S. Desikan, F. Ségonne, B. Fischl, B. T. Quinn, B. C. Dickerson, D. Blacker, R. L. Buckner, A. M. Dale, R. P. Maguire, B. T. Hyman, M. S. Albert, R. J. Killiany, *Neuroimage* **2006**, *31*(3), 968. https://doi.org/10.1016/j.neuroimage.2006.01.021.
[23] J. E. Iglesias, J. C. Augustinack, K. Nguyen, C. M. Player, A. Player, M. Wright, N. Roy, M. P. Frosch, A. McKee, L. L. Wald, B. Fischl, K. van Leemput, Alzheimer's Disease Neuroimaging Initiative, *Neuroimage* **2015**, *115*, 117. https://doi.org/10.1016/J.NEUROIMAGE.2015.04.042.
[24] G. FRENS, *Nat. Phys. Sci.* **1973**, *241*(105), 20. https://doi.org/10.1038/physci241020a0.
[25] P. C. Lee, D. Meisel, *J. Phys. Chem.* **1982**, *86*(17), 3391. https://doi.org/10.1021/j100214a025.
[26] A. Bonifacio, S. Dalla Marta, R. Spizzo, S. Cervo, A. Steffan, A. Colombatti, V. Sergo, *Anal. Bioanal. Chem.* **2014**, *406*(9–10), 2355. https://doi.org/10.1007/s00216-014-7622-1.
[27] D. Zhang, S. M. Ansar, K. Vangala, D. Jiang, *J. Raman Spectrosc.* **2010**, *41*(9), 952. https://doi.org/10.1002/jrs.2548.
[28] A. I. Henry, J. M. Bingham, E. Ringe, L. D. Marks, G. C. Schatz, R. P. Van Duyne, *J. Phys. Chem. C* **2011**, *115*(19), 9291. https://doi.org/10.1021/jp2010309.
[29] M. Kahraman, S. Wachsmann-Hogiu, *Anal. Chim. Acta* **2015**, *856*, 74. https://doi.org/10.1016/j.aca.2014.11.019.
[30] T. H. Kang, T. Friedmann, *Neurosci Lett.* **2015**, *590*, 35. https://doi.org/10.1016/J.NEULET.2015.01.042.
[31] S. M. Euser, A. Hofman, R. G. J. Westendorp, M. M. B. Breteler, *Brain* **2008**, *132*(2), 377. https://doi.org/10.1093/brain/awn316.
[32] A. Tramutola, C. Lanzillotta, M. Perluigi, D. A. Butterfield, *Brain Res Bull* **2017**, *133*, 88. https://doi.org/10.1016/j.brainresbull.2016.06.005.
[33] R. Gautam, S. Vanga, F. Ariese, S. Umapathy, *EPJ Tech. Instrum.* **2015**, *2*, 8. https://doi.org/10.1140/epjti/s40485-015-0018-6.
[34] D. C. Wang, C. H. Sun, L. Y. Liu, X. H. Sun, X. W. Jin, W. L. Song, X. Q. Liu, X. L. Wan, *Neurobiol. Aging* **2012**, *33*(6), 1057. https://doi.org/10.1016/j.neurobiolaging.2010.09.013.
[35] A. A. Ziegenhorn, O. Schulte-Herbrüggen, H. Danker-Hopfe, M. Malbranc, H. D. Hartung, D. Anders, U. E. Lang, E. Steinhagen-Thiessen, R. T. Schaub, R. Hellweg, *Neurobiol. Aging* **2007**, *28*(9), 1436. https://doi.org/10.1016/j.neurobiolaging.2006.06.011.
[36] H. Geekiyanage, G. A. Jicha, P. T. Nelson, C. Chan, *Exp. Neurol.* **2012**, *235*(2), 491. https://doi.org/10.1016/j.expneurol.2011.11.026.
[37] R. E. Mrak, W. S. T. Griffin, *J. Alzheimers Dis.* **2006**, *8*(4), 369. https://doi.org/10.3233/JAD-2005-8406.
[38] O. Preische, S. A. Schultz, A. Apel, et al., *Nat. Med.* **2019**, *25*(2), 277. https://doi.org/10.1038/s41591-018-0304-3.
[39] T. Miura, C. Yamamiya, M. Sasaki, K. Suzuki, H. Takeuchi, *J Raman Spectrosc.* **2002**, *33*(7), 530. https://doi.org/10.1002/jrs.869.
[40] E. B. Hanlon, I. Itzkan, R. R. Dasari, et al., *Photochem. Photobiol.* **1999**, *70*(2), 236. http://www.ncbi.nlm.nih.gov/pubmed/10461462 Accessed October 14, 2019.
[41] P. Chen, A. Shen, W. Zhao, S.-J. Baek, H. Yuan, J. Hu, *Appl. Optics* **2009**, *48*(24), 4743. https://doi.org/10.1364/ao.48.004743.
[42] E. Ryzhikova, N. M. Ralbovsky, L. Halámková, D. Celmins, P. Malone, E. Molho, J. Quinn, E. A. Zimmerman, I. K. Lednev, *Appl. Sci.* **2019**, *9*(16), 3256. https://doi.org/10.3390/app9163256.
[43] M. S. Albert, S. T. DeKosky, D. Dickson, et al., *Alzheimers Dement.* **2011**, *7*(3), 270. https://doi.org/10.1016/J.JALZ.2011.03.008.
[44] B. Olsson, R. Lautner, U. Andreasson, A. Öhrfelt, E. Portelius, M. Bjerke, M. Hölttä, C. Rosén, C. Olsson, G. Strobel, E. Wu, K. Dakin, M. Petzold, K. Blennow, H. Zetterberg, *Lancet Neurol.* **2016**, *15*(7), 673. https://doi.org/10.1016/S1474-4422(16)00070-3.

SUPPORTING INFORMATION

Additional supporting information may be found online in the Supporting Information section at the end of this article.

How to cite this article: Carlomagno C, Cabinio M, Picciolini S, Gualerzi A, Baglio F, Bedoni M. SERS-based biosensor for Alzheimer disease evaluation through the fast analysis of human serum. *J. Biophotonics*. 2020;13:e201960033. https://doi.org/10.1002/jbio.201960033